Supplementary Material

Imaging parameters of the 3T example patient

Presurgical imaging was performed on a 3T MRI system (Skyra Magnetom, Siemens, Erlangen, Germany). The patient was not sedated for imaging. For better visualization of vascular structures, a standard dose of 0.1 mmol/kg gadobutrol was administered intravenously at the start of the procedure. The MRI protocol consisted of the following sequences: head scout (14 s), sagittal 3D T1-weighted gradient-echo sequence (MPRAGE; TR/TE/TI 2300/2.32/900 ms, voxel size 0.9 × 0.9 × 0.9 mm^3, FOV 240 × 240 mm^2; 5 min. 21 s), axial T2 TSE (TR/TE 13320/101 ms, voxel size 0.7 × 0.7 × 2.0 mm^3, FOV 250 × 250 mm^2; 3 min. 48 s), sagittal Fast Grey Matter Acquisition T1 Inversion Recovery (FGATIR; TR/TE/TI 1500/3.56/559 ms, voxel size 0.8 × 0.8 × 1.0 mm^3, FOV 240 × 240 mm^2; 6 min. 17 s), axial proton-weighted TSE (TR/TE 3600/11 ms, voxel size 1.0 × 1.0 × 2.0 mm^3, FOV 250 × 250 mm^2; 3 min. 34 s), and dMRI (EPI, TR/TE 7500/95 ms, voxel size 2.0 × 2.0 × 2.0 mm^3, FOV 250 × 250 mm^2, 20 diffusion-encoding directions with b-value 1000 s/mm^2 and one non-diffusion-weighted b_0-volume; 5 min. 47 s). Overall acquisition time was 25 min. A routine head CT was done the day after electrode implantation using an 80-multislice Toshiba Aquilion PRIME (Canon Medical Systems, Otawara, Japan). Four sequential blocks, each with a length of 37.75 mm, were acquired (280 mA, 120 kV, rotation time 1 s, matrix 512 x 512 mm^2, $CTDI_{vol}$ 55.79 mGy), resulting in a slice thickness of 0.5 mm.

Imaging parameters of the retrospective 1.5T cohort

All patients underwent pre-operative MR-imaging on a 1.5 T scanner (NT Intera; Philips Medical Systems, Best, The Netherlands) using a T2-weighted fast spin-echo (FSE) with the following parameters: TR = 3500 ms, TE = 138 ms, echo-train length: 8, excitations: 3, flip angle: 90°, section thickness: 2 mm, section gap: 0.2 mm, FOV: 260 mm (in-plane resolution 0.51 × 0.51 mm), matrix size: 384 interpolated to 512, total acquisition time, 10 min and 41 s.

Postoperative MR-imaging was performed in 45 patients. DBS patients are subject to a limitation of the specific absorption rate (SAR, b0.1 W/kg), which has been specified by the manufacturer of the electrodes. Within 5 days after implantation of the electrodes, MR-imaging was performed on the same scanner using a T2-weighted fast spin-echo (FSE) sequence in low SAR mode with the same parameters as used pre-operatively. Philips software Version 11.1 level 4 was used. MR sections in the axial and coronal planes were

obtained and processed in this study. In the following, “axial” and “coronal” volumes refer to acquisitions with voxel sizes of 0.51 × 0.51 mm in the axial or coronal planes respectively, each with a 2 mm slice thickness. Postoperative CT was conducted in 6 patients (8 of whom also had postoperative MRI). Here, high-resolution images were acquired on a LightSpeed16 (GE Medical System, Milwaukee, Wisconsin) Slice CT with a spatial resolution of 0.49 × 0.49 × 0.67 mm^3. Images were acquired in axial (i.e. sequential/incremental) order at 140 kV and automated mA setting. Noise index was 7.0. A large SFOV with 50 cm diameter was used.

Methodological details for normalization strategies as implemented in Lead-DBS

SPM Unified Segmentation

In Lead-DBS, the Unified Segmentation approach does not fit warps to the standard tissue probability maps (TPM) supplied with SPM software which are based on a population differing from the original MNI-152 population (IXI-Dataset; http://brain-development.org/ixi-dataset/). Instead, the multispectral (T1-, T2-, PD-weighted) MNI-152 / ICBM 2009b Nonlinear Asymmetric template series were preprocessed using the Unified Segmentation approach, generating a new set of templates. Moreover, this was done using refined tissue priors that include subcortical structures and have been proposed for use in the DBS context (Lorio et al., 2016). This procedure ensures direct compatibility with the 2009b space (Fonov et al., 2009) and the use of these adapted TPM yielded slightly better segmentations of STN and GPi in a recent comparison (Ewert et al., 2018a). Of note, all implementations of SPM methods (Unified Segmentation, DARTEL & SHOOT, see below) within Lead-DBS by default operate on all preoperative acquisitions simultaneously (multispectral normalization).

SPM DARTEL & SHOOT

SPM DARTEL/SHOOT create population-specific group average templates based on the data available (Ashburner, 2007; Ashburner and Friston, 2011). As these are different to MNI space, we adapted the pipeline to register to single subjects directly to MNI space derived from the multispectral 2009b data described above.

Advanced Normalization Tools (ANTs)

ANTs is another non-linear pipeline that has been extensively optimized for LEAD-DBS 2.0 (Ewert et al., 2018a). The current default implementation is a multispectral warp that

combines a rigid, an affine and two nonlinear symmetric image normalization (SyN) stages. While the first SyN stage includes the whole brain, the second is limited to a subcortical region mask defined in (Schönecker et al., 2009). The implementation detects and properly handles slabs, which are often used in clinical context. For instance, many centers acquire whole-brain 3D gradient-echo T1-weighted series and a T2-weighted slab of the subcortex for stereotactic planning (Horn et al., 2017c). If slabs are detected, Lead-DBS automatically adds a third intermediate SyN stage that focuses on the area covered by all acquisitions (whereas the linear stages and first SyN stage only takes the whole-brain acquisition(s) into account).

MAGeT Brain-like Segmentation

The MAGeT Brain approach (https://github.com/CobraLab/MAGeTbrain; Chakravarty et al., 2012) was developed for segmentation of deep nuclei and computes multiple warps from atlas space via multiple “templates” to the subject of question. Here, templates refer to additional brains (e.g. high resolution MRIs acquired on specialized hardware). Thus, the deformation from atlas to subject space takes “detours” via multiple different brains and, as a result, multiple solutions for the atlas based segmentation are attained. These solutions are then aggregated (e.g. by simple averaging or majority voting). The intuitive understanding of the approach is that it increases robustness by introducing anatomical variance and the original authors showed this increased precision empirically in multiple studies (Chakravarty et al., 2012; Pipitone et al., 2014).

In Lead-DBS, this concept is adopted and used for both segmentation and normalization. In a first step, key structures defined by the DISTAL atlas in 2009b space (STN, GPi, GPe, RN) are segmented in native space using an adapted MAGeT Brain approach implemented in Lead-DBS using ANTs. In a second step, a SyN-based ANTs-registration from native to template space is computed (see above) that additionally includes the segmented labels as further “spectra” in the warp. For example, if preoperative T1- and T2-weighted acquisitions are present, a six-fold normalization is computed (including T1-patient to T1-MNI, T2-patient to T2-MNI, auto-segmented patient STN to DISTAL atlas STN, patient GPi to DISTAL GPi, etc.). This approach may add additional precision at and around key interest regions in DBS but has not been empirically tested or compared to conventional approaches beyond the original MAGeT publications (Chakravarty et al., 2012; Pipitone et al., 2014).

MAGeT Brain-like Normalization

This further adaptation of the MAGeT Brain approach reverses the idea and directly works on the deformation fields solved during normalization. Specifically, multiple deformation fields warping from subject to template are created, each taking a detour via a peer brain ("template" in the MAGeT-Brain nomenclature). Resulting deformation fields are then aggregated by calculating their voxel-wise robust average. A final deformation field that warps from subject to template space is created that can be applied to warp electrodes into template space. Of note, both MAGeT-inspired methods require the use of "peer-subjects" to include into the analysis. To demonstrate this in the present patient example, 21 age-matched peers from the IXI-dataset (http://brain-development.org/ixi-dataset/) were automatically assigned by Lead-DBS as previously described in similar context (Horn et al., 2017a).

Methodological details for volume of tissue activated generation

Mesh Generation

A cylindrical four-compartment model of the area surrounding the electrode and the lead itself is constructed based on the conducting and insulating parts of the electrodes, gray matter, and white matter. This model is represented by a tetrahedral mesh that is generated using the iso2mesh toolbox (http://iso2mesh.sourceforge.net/) in combination with other meshing tools, including Tetgen (http://wias-berlin.de/software/tetgen/) for the Delaunay tetrahedralization step and Cork (https://github.com/gilbo/cork) for merging electrode and brain surface meshes. We note here that all involved tools are included within Lead-DBS and some interfaces of iso2mesh were slightly modified. The output mesh is truncated by a cylindrical boundary with a radius of 20 mm; a larger radius is automatically used when higher stimulation amplitudes are applied. All regions within the cylinder not covered by either gray matter or the electrode are modeled as isotropic white matter. Gray matter portions are defined by the atlas chosen by the user (table 5). This gray matter model can be either informed by an atlas available in template space, the same atlas that was automatically transferred to native space or a manual segmentation of structures of interest manually performed by the user.

Finally, the conducting and insulating regions are specified by the electrode models supplied with Lead-DBS. A wide range of electrodes from five manufacturers are readily implemented in Lead-DBS (table 7) and it is straight forward to implement custom models.

Surface meshes from electrode and atlas as well as the bounding cylinder are resolved to a joint surface mesh using a modified version of Cork as implemented in iso2mesh. This joint mesh is then fed into Tetgen to create a tetrahedral mesh. Tetrahedra within the regions of gray matter, white matter, metal or insulating parts are identified and tagged using a post-processing code implemented in Lead-DBS.

Electric Field Modeling using Finite Element Method (FEM)

Conductivity at each tetrahedron is estimated using the FieldTrip / SimBio pipeline (Oostenveld et al., 2010; Vorwerk et al., 2014; 2018; https://www.mrt.uni-jena.de/simbio/; http://www.fieldtriptoolbox.org/). Conductivity values for gray and white matter can be entered by the user while two presets are available. The first consists of conductivity values commonly used in the field (0.33 and 0.14 S/mm for gray and white matter, respectively). Similar values were used in modeling EEG data (e.g. Buzsáki, 2006; Vorwerk et al., 2014) and in most previous DBS models (e.g. Åström et al., 2014; McIntyre and Grill, 2002). However, these conductivity values are not corrected for stimulation frequency and drop drastically at a typical stimulation frequency of 130 Hz (Hasgall et al., 2015). Thus, a second set of conductivity presets adjusted for stimulation frequency is available (0.0915 and 0.059 S/mm).

Both constant-voltage and constant-current settings can be modeled. The voltage or amplitude applied to the active contacts is introduced as a boundary condition. In case of monopolar stimulation, the surface of the bounding cylinder serves as the anode. Subsequently, the gradient of the potential distribution is calculated by derivation of the FEM solution. Due to the first order FEM approach that is used, the resulting gradient is piecewise continuous. The binary VTA is obtained by thresholding the resulting electric field strength at a user-specified value. In the past, a value of 0.2 V/mm has frequently been used in this context (Åström et al., 2014; 2009; Horn et al., 2017c; Vasques et al., 2009). In Lead-DBS, this value serves as the “general heuristic” default value. Furthermore, based on prior literature, heuristics for STN (0.19 V/mm; Åström et al., 2014; Mädler and Coenen, 2012), GPi (0.2 V/mm; Hemm et al., 2005; Vasques et al., 2009) and Vim (0.165 V/mm; Åström et al., 2014; Kuncel et al., 2008) can be used. Finally, specific activation thresholds that depend on axon diameters (D = 2-5 µm) and stimulation pulse-widths (t = 30, 60, 90, 120 µs) are available as they were estimated in (Åström et al., 2014).

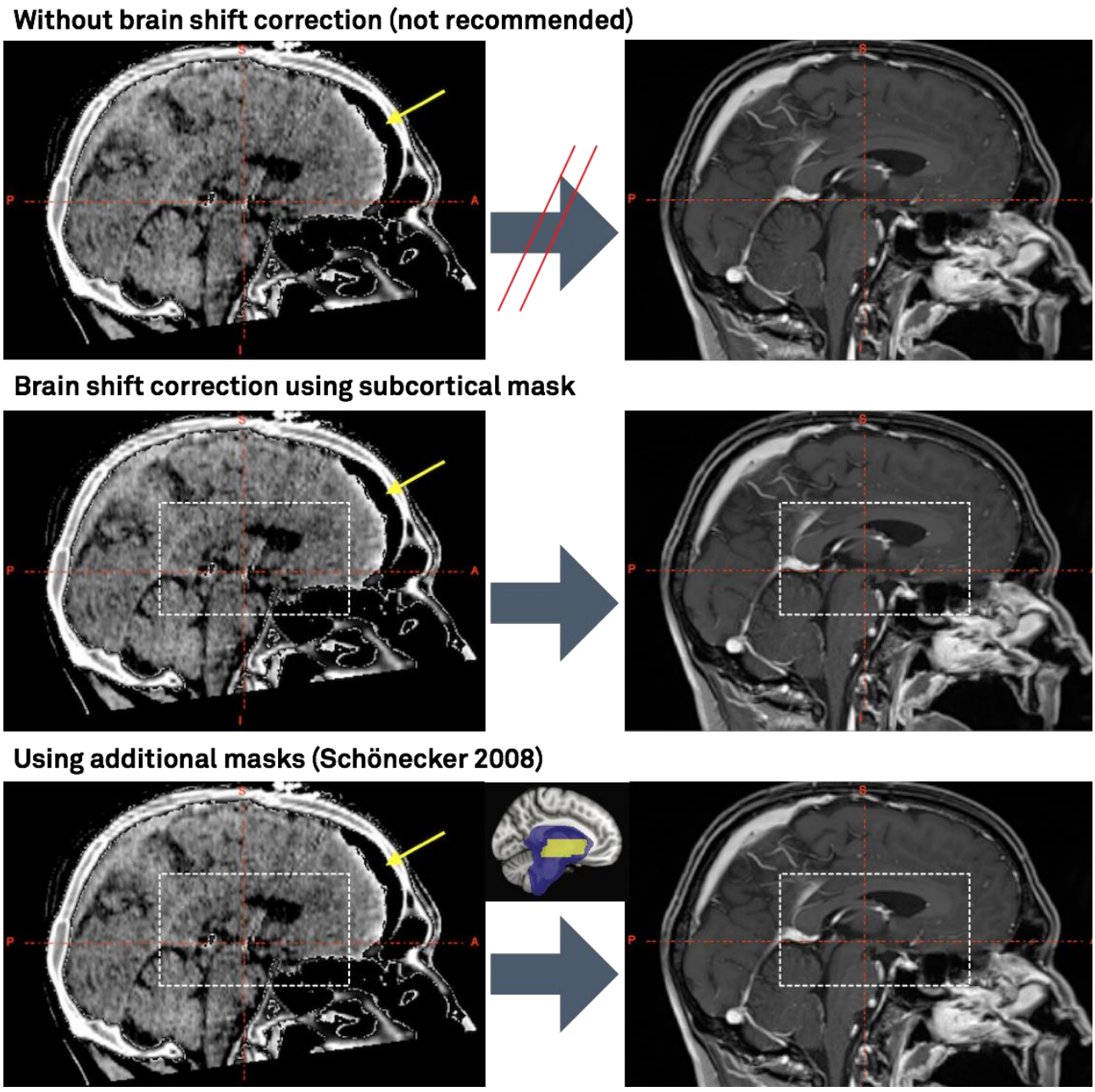

Figure S1: Brain shift correction approach. The top panel shows a whole-brain affine registration aligning a postoperative CT with frontal pneumocephalus (left) to a preoperative T1-weighted MRI (post gadolinium). Based on the pneumocephalus (yellow arrow), a nonlinear error results that is largest in frontal regions (at the site of the pneumocephalus) that may still be substantial in the regions of interest of DBS (figure 5). In the mid row, an additional refinement transform between the subcortical area delineated by the white dashed box is computed. Finally, in the third row, one or two additional refinement transforms between subcortical areas of interest are computed based on masks defined in (Schönecker et al., 2009). This approach gradually shifts the registration area away from the area nonlinearly distorted by pneumocephalus toward the subcortical regions of interest.